

EBG Structures Properties and their Application to Improve Radiation of a Low Profile Antenna

Masoumeh Rezaei Abkenar

Department of Electrical and Computer Engineering, Semnan University
m_rezaie83@yahoo.com

Pejman Rezaei*

Department of Electrical and Computer Engineering, Semnan University
prezaei@semnan.ac.ir

Received: 24/Nov/2012

Accepted: 11/Dec/2013

Abstract

In this paper we have studied the characteristics of mushroom-like Electromagnetic Band Gap (EBG) structure and performance of a low profile antenna over it. Afterward, a novel EBG surface is presented by some modifications in mushroom-like EBG structure. This structure, which has more compact electrical dimensions, is analyzed and its electromagnetic properties are derived. Results show that resonant frequency of this novel structure is about 15.3% lower than the basic structure with the same size. Moreover, the novel EBG structure has been used as the ground plane of antenna. Its application has improved radiation of a low profile dipole antenna. The antenna performance over the new EBG ground plane is compared with the conventional mushroom-like EBG structure. Simulation results show that using this slot loaded EBG surface, results in 13.68dB improvement in antenna return loss, in comparison with conventional mushroom-like EBG, and 33.87dB improvement in comparison with metal ground plane. Besides, results show that, EBG ground planes have increased the input match frequency bandwidth of antenna.

Keywords: Electromagnetic Band Gap (EBG), Low Profile Antenna, Slot Loaded EBG Surface, Bandwidth, Dipole Antenna.

1. Introduction

In the last two decades, artificial periodic structures have been used in a wide range of engineering applications. Electromagnetic Band Gap (EBG) structures are a group of these artificial periodic structures, and recently their application in different antennas has attracted much research interests in electromagnetic applications. EBG structures are a novel class of artificially fabricated structures, and can control the propagation of electromagnetic waves inside themselves. These structures have two important and special electromagnetic properties. The first one is suppression of surface waves in a specific frequency band, which called the band gap. The other one is phase response to the plane wave illumination; these structures have a reflection phase that changes vs. frequency from 180° to -180° [1]. Besides, these structures possess some other exciting features, like high impedance in their performance band. According to these properties, a wide range of applications have been reported, such as TEM waveguides, different microwave filters and low profile wire antennas [2-5].

Mushroom-like EBG structure initially designed by D. Sievenpiper [6] is a popular structure that exhibits compactness and simple implementation features compared to other EBG structures. This conventional mushroom-like EBG can be used in different antenna

designs to suppress surface waves. But in some practical applications smaller cell size is needed.

In this paper, at first we have studied the features of a mushroom-like EBG structure. Then, a novel structure is designed by inserting some slots in the patches of mushroom-like EBG cells. These slots significantly enlarge capacitance of equivalent LC circuit and so result in a more compact structure. Electromagnetic properties of the new slot loaded EBG is derived and compared with conventional mushroom-like EBG. Additionally, to study the effect of the EBG structures, performance of a low profile antenna over these structures has been observed. We have utilized both EBG structures as ground planes to improve the radiation efficiency of a dipole antenna near the ground plane. Also, performance of antenna has been compared with an antenna over Perfect Electric Conductor (PEC) ground plane.

A considerable improvement in antenna performance has been observed.

The structure was analyzed in our previous works [7-10] by Ansoft HFSS, which is a commercially available simulation tool based on finite element method [11]. In this paper the dispersion diagram of the structure is also derived by CST Microwave Studio [12], and the result are in agreement with previous results.

* Corresponding Author

2. Surface Waves

In this section we want to study surface waves and the conditions in which they can occur. Surface waves are the waves which can exist on the interface between any two dissimilar materials, like metal and free space. They are strongly bounded to the surface, and their fields exponentially decay along normal direction to the surface [13]. Surface waves are an important issue for many antennas, since these waves propagate along the ground plane instead of radiation into free space, so reduce the antenna efficiency and gain.

To derive the characteristics of surface waves on the interface between a material and free space, assume the surface is in the YZ plane, free space extending in the +X direction, and the other material in the -X direction. This configuration is shown in Figure 1.

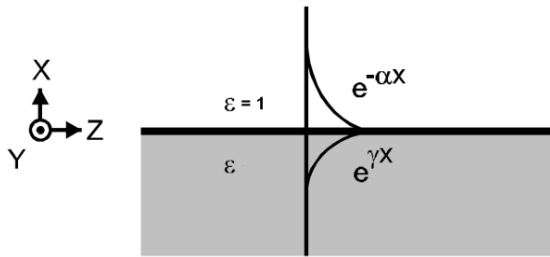


Fig. 1 A surface wave on the interface of a material and free space.

The surface wave decays in the +X direction with decay constant α , and in the -X direction with decay constant γ . By combining electromagnetic fields in two materials according to Maxwell's equations, decay constants α and γ for a TM surface wave are derived as (1) and (2) [14,15]:

$$\alpha = \sqrt{-1/(1+\varepsilon)} \omega/c \quad (1)$$

$$\gamma = \sqrt{-\varepsilon^2/(1+\varepsilon)} \omega/c \quad (2)$$

For a positive ε , decay constants are imaginary, and the waves do not decay as the distance from the surface increases. Thus, these waves are plane waves that propagate through the dielectric interface. On the other hand, when ε is less than -1, or when it is imaginary, the solution shows a wave that is bound to the surface. Therefore, TM mode surface waves can exist only on the metals, or other materials with non-positive dielectric constants. By exchanging the electric and magnetic fields and substituting ε with μ , according to the principle of duality, above expressions can be applied to the TE mode [16].

From the other point of view we can consider the surface impedance of surface, which is defined as the ratio of the electric field over the magnetic field. For the above surface in the YZ plane, required surface impedance for TM surface waves is obtained as below by considering electric and magnetic fields on the surface [14,17]:

$$Z_s(TM) = \frac{E_z}{H_y} = \frac{j\alpha}{\omega\varepsilon} \quad (3)$$

So TM waves only can occur on a surface with positive reactance that means inductive surface impedance. For a TE wave the surface impedance is equal to the following expression:

$$Z_s(TE) = \frac{E_z}{H_y} = -\frac{j\omega\mu}{\alpha} \quad (4)$$

Thus, a negative reactance is necessary for TE surface waves, it means capacitive surface impedance.

3. Reflection Phase

The Reflection phase is an important property of EBG structures, which is determined as the phase of reflected electric field at the reflecting surface. In EBG structures it varies with frequency from 180° to -180° . So in a specific frequency band, when the reflection phase is around 0° , they can be used as proper ground planes, like Perfect Magnetic Conductors (PMC).

For a surface in the YZ plane, the surface impedance seen by an incident wave in the X direction is equal to:

$$Z_s = E_z / H_y \quad (5)$$

For a high impedance surface, the ratio in Equation (5) is too high, so the electric field has a non-zero value, while the magnetic field is zero. In the other word, this surface is called a magnetic conductor, because of its zero tangential magnetic fields at the surface.

The reflection phase is the phase difference between the backward and forward waves which formed a standing wave on an arbitrary surface. The electromagnetic fields on the surface are expressed as (6) and (7). Besides, the boundary condition at the surface is given by the surface impedance as (8) [18]:

$$E(x) = E_f e^{-jkx} + E_b e^{jkx} \quad (6)$$

$$H(x) = H_f e^{-jkx} + H_b e^{jkx} \quad (7)$$

$$\frac{E_{total}(x=0)}{H_{total}(x=0)} = Z_s \quad (8)$$

Moreover, the electric and magnetic fields of each wave are related by means of the impedance of free space as (9).

$$\left| \frac{E_f(x)}{H_f(x)} \right| = \left| \frac{E_b(x)}{H_b(x)} \right| = \sqrt{\frac{\mu_0}{\varepsilon_0}} = \eta \quad (9)$$

And the reflection phase is equal to:

$$\Phi = \text{Im} \left\{ \ln \left(\frac{E_b}{E_f} \right) \right\} \quad (10)$$

Combining Equation (8), (9) and (10) gives the reflection phase of a surface with impedance Z_s :

$$\Phi = \text{Im} \left\{ \ln \left(\frac{Z_s - \eta}{Z_s + \eta} \right) \right\} \quad (11)$$

As a result when Z_s has a low value, like a PEC surface, the reflection phase will be $\pm \pi$, and when it is very high, like an EBG surface, the reflection phase will be zero.

4. EBG Structures Design and Characterization

4.1 Mushroom-Like EBG

As previously mentioned, mushroom-like EBG structure is one of the basic and most common EBG structures. This structure is shown in Figure 2. It consists of a flat metal sheet that is covered with an array of metal protrusions on a dielectric substrate which are connected to the lower conducting surface by metal vias [6]. The parameters of the EBG structure are labeled as patch width w , gap width g , substrate thickness h , dielectric constant ϵ_r , and vias radius r . When the periodicity of structure, which is equal to $w+g$, is small compared to the operating wavelength, the operation mechanism of structure can be explained using an effective medium model with equivalent lumped LC elements, as explained in [18]. The capacitor C , results from the gap effect between the patches and the inductor L , due to the current flowing along adjacent patches. Thus, the surface impedance and central frequency of band gap are estimated like a parallel resonant circuit:

$$Z = \frac{j\omega L}{1 - \omega^2 LC} \tag{12}$$

$$\omega_0 = 1/\sqrt{LC} \tag{13}$$

It is clear that, at low frequencies surface impedance of the structure is inductive, so it supports TM surface waves. Inversely, it is capacitive at high frequencies, and supports TE surface waves. Around the LC resonance frequency, the impedance is very high. In this frequency band the structure suppresses propagation of both TE and TM modes of surface waves. Also, it reflects incident electromagnetic waves without phase reversal that occurs on a PEC. This frequency band is called the band gap.

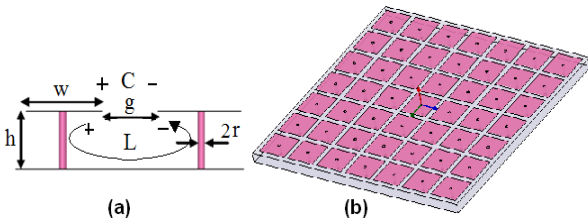


Fig. 2 Mushroom-like EBG, a) unit cell, b) 3D view.

4.2 Slot Loaded EBG

Since Slot loaded EBG is a new type of EBG structures which are designed by cutting some slots into the metal patches of conventional mushroom-like EBG. These slots change the current flow on the patches which caused to a longer current path. They also create extra capacitance between the slot edges. So the values of L

and C in (1) are increased and result in a lower frequency band gap and finally a more compact structure [19-23].

In this paper we have designed a novel slot loaded EBG structure by cutting a pair of I-like, X-oriented slots into the patch of a mushroom-like EBG cell. The structure is shown in Figure 3. Dimensions of the basic mushroom-like cell are designed as: $w=3\text{mm}$, $g=0.5\text{mm}$, $h=1\text{mm}$ and $r=0.125\text{mm}$. A dielectric layer with $\epsilon_r=2.33$ is used as substrate. Lengths of slots are optimized to obtain the most compact structure. Finally, dimensions of slots are designed as: $L_1=1.5\text{mm}$, $L_2=1\text{mm}$, $L_3=0.5\text{mm}$ and $L_4=0.25\text{mm}$.

The initial inductance and capacitance of the mushroom-like EBG structure are [18]:

$$L = \mu_0 \mu_r h \tag{14}$$

$$C = \frac{W \epsilon_0 (1 + \epsilon_r)}{\pi} \cosh^{-1} \left(\frac{W + g}{g} \right) \tag{15}$$

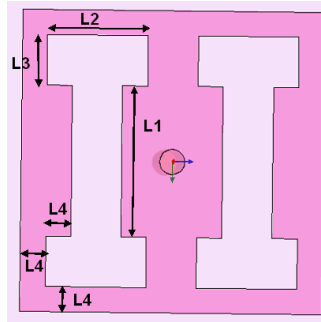


Fig. 3 Unit cell of the designed EBG cell.

The equivalent inductance and capacitance of the new structure are equal to the above initial inductance and capacitance, in addition to the new inductance and capacitance which are created by slots. So by inserting the slots, the initial value of L and C remain unchanged, while the equivalent L and C will increase, and result in a lower resonant frequency. Thus, the wavelength will increase and the electrical dimensions of the EBG cell, which mean the dimensions in comparison to the wavelength, will decrease. Thus, we will achieve to a more compact EBG cell. In next section we will study this structure's properties, and it will be compared with the basic structure.

4.3 Characterization of EBG Structures

4.3.1 Reflection Phase Diagram

As it is mentioned in previous sections, reflection phase is one of the most important characteristics of EBG structures. To extract the reflection phase diagram in HFSS, a unit cell is modeled and periodic boundary conditions are applied on side walls. This structure is shown in Figure 4. The cell is excited by a plane wave in different frequencies and phase of the reflected wave at evaluation plane is calculated as [24]:

$$\Phi_{\text{EBG}} = \frac{\int_S \text{Phase}(E_{\text{scattered}}) ds}{\int_S ds} \tag{16}$$

In the above expression, S is the evaluation plane.

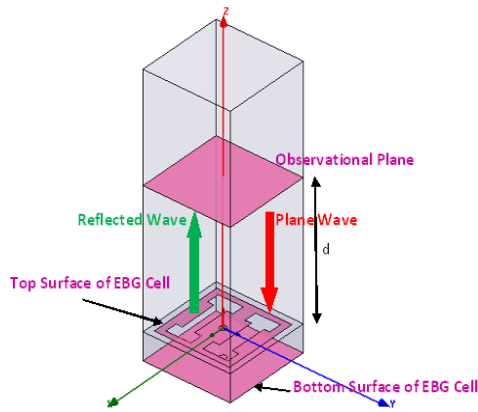


Fig. 4 Simulated cell to extract reflection phase.

The reflection phase diagrams of a normally incident plane wave on the conventional mushroom-like EBG and the new slot loaded EBG are obtained by this method and shown in Figure 5.

In antenna applications, it has been shown practically that the desired band for antenna radiation on an EBG plane is close to the frequency region where the EBG surface has a reflection phase in the range of $90^\circ \pm 45^\circ$ [25]. The $90^\circ \pm 45^\circ$ criterion is also compatible to PEC and PMC planes. PEC surface has 180° reflection phases for a horizontally positioned dipole antenna, and reverse image current decreases the antenna radiation performance, while a PMC surface has 0° reflection phase. Hence, when the EBG ground plane exhibits a reflection phase in the middle of this region, a good return loss is expected for the dipole antenna.

According to Figure 5, $90^\circ \pm 45^\circ$ frequency band and in-phase (zero degree) reflection frequency of mushroom-like and slot loaded EBG structures are shown in Table 1. So the in-phase reflection frequency of novel slot loaded EBG is 15.3% lower than mushroom-like EBG of the same size, and decreases from 17GHz to 14.4GHz, since the slots affect the electric currents flowing along the patch and result in a longer current path [18].

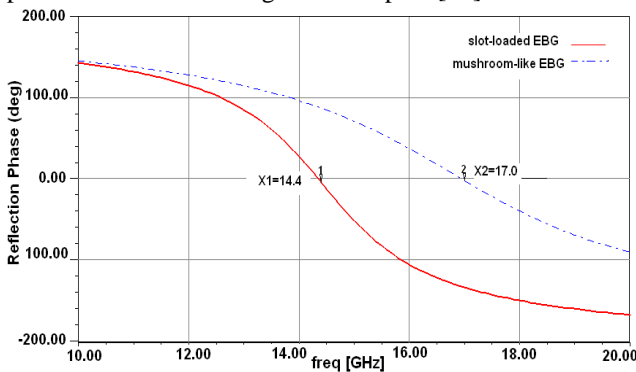


Fig. 5 Reflection phase of a normally incident plane wave with Ex polarization on the two types of EBG structures.

Table 1: $90^\circ \pm 45^\circ$ frequency band and in-phase reflection frequency of mushroom-like and slot loaded EBG structures

Structure Types	Reflection Phase Specifications [GHz]		
	f _l	f _h	f ₀
Mushroom-like EBG	11.3	15.8	17
Slot loaded EBG	10.8	13.8	14.4

According to Table 1 the period of mushroom-like and slot loaded EBG structures at their in-phase reflection frequency, f₀, and central frequency of $90^\circ \pm 45^\circ$ region, f_c, is calculated and shown in Table 2. It represents that the slot loaded EBG surface has smaller cell size at different operation frequencies.

Table 2: Period of EBG structures

Structure Types	Period of Structure [λ]	
	f ₀	f _c
Mushroom-like EBG	$0.198 \lambda_0$	$0.158 \lambda_c$
Slot loaded EBG	$0.168 \lambda_0$	$0.144 \lambda_c$

On the other hand, the results show that if we increase the patch size of mushroom-like EBG cell to 3.85mm, the structure will operate at the same frequency band to the slot loaded EBG surface. In this case the period of structure is $P=w+g=4.35\text{mm}$, so the new slot loaded EBG cell size is reduced by 20%. This structure's reflection phase is shown in Figure 6.

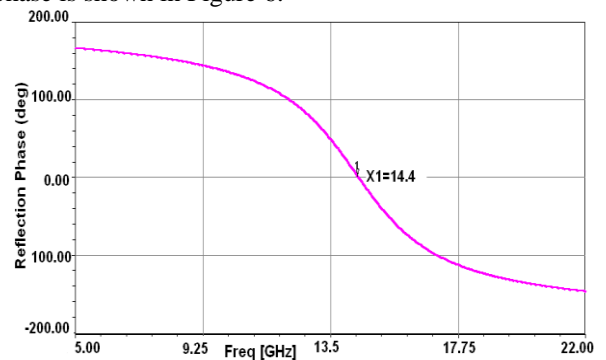


Fig. 6 Reflection phase of a Mushroom-like EBG cell with $w=3.85\text{mm}$.

4.3.2 Dispersion Diagram Method

The Dispersion diagram or β -f, curve is the other important characteristic of EBG structures, and can be calculated from the unit cell and applying a periodic boundary condition with appropriate phase shifts on the sides. According to Floquet theorem and its expansion by Bloch, dispersion curve is periodic. Therefore, we only need to plot the dispersion relation within one single period, which is known as the Brillouin zone. The smallest region within the Brillouin zone for which the directions are not related by symmetry is called the irreducible Brillouin zone. The irreducible Brillouin zone of our structure is a triangular wedges with 1/8 the area of the full Brillouin zone defined by Γ , X and M points [26]. The simulated cell by CST Microwave Studio [12], is depicted in Figure 7.

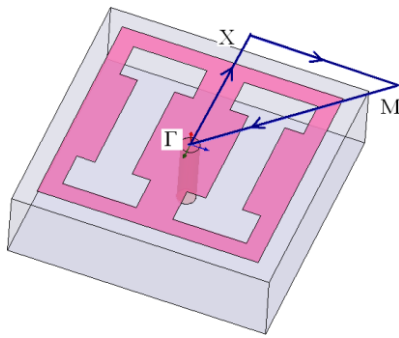


Fig. 7 The simulated cell to extract dispersion diagram.

Two dimensional Eigen mode solutions for Maxwell's equations are solved for the Brillouin zone. As it can be seen in Figure 8, the band gap of dispersion curve for the mushroom-like EBG is between 11.48-16.14GHz, while for the slot-loaded EBG it is about 10.81-15.30GHz frequency band. Thus, the novel slot-loaded EBG has a band gap in a lower frequency band, in comparison to the mushroom-like EBG.

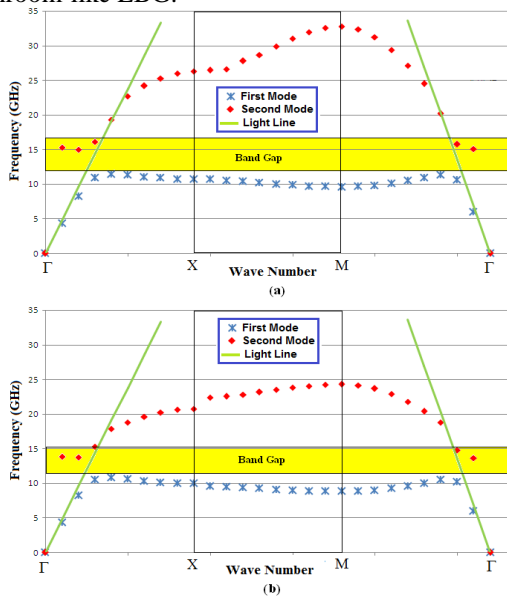


Fig. 8 Dispersion diagram, a) mushroom-like EBG, b) slot loaded EBG.

4.3.3 Direct Transmission Method

The other method to determine the band gap of EBG structure is direct transmission. In this method wave transmission through EBG structure is modeled as scattering parameter S21. As it is shown in Figure 9, a part of structure which is repeated in different directions of the lattice is considered as a TEM waveguide with two pairs of parallel PEC and PMC sides [27].

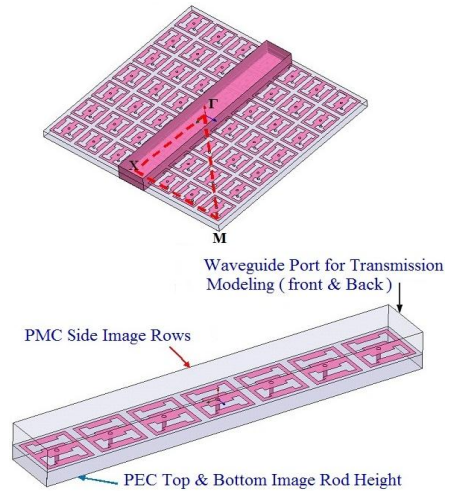


Fig. 9 The simulated TEM waveguide in direct transmission method.

We excite it with two ports on remained sides, and the transmission coefficient between these two ports can show the band gap. But this method is appropriate just for symmetric structures and along the propagation direction. In this paper we have used a 7x7 lattice of mushroom-like and the slot loaded cells near antenna. So we have a 1x7 lattice as a TEM waveguide. The transmission diagram of these structures is shown in Figure 10. The desired frequency band usually is considered as the region where S21 has the value less than -20dB.

According to Figure 10, the band gap of mushroom-like EBG is 10.39-15.73GHz, while it is 10.06-14.07GHz for the slot loaded EBG. Hence, it is clear that the band gap region of the novel structure is decreased based on direct transmission method too.

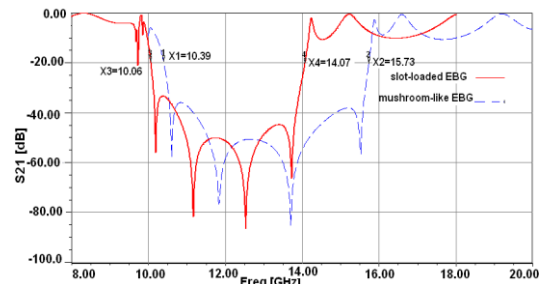


Fig. 10 Comparison of S21 for mushroom-like and slot loaded EBG.

In this section, the EBG structure is analyzed with three methods. Because of the different nature of these methods, the results are not necessarily the same. In fact each of them is measuring a different property of the structure, and depending on the application one of them will be more useful. For example when the structure is used as the ground plane for a wire antenna, we want to have in phase reflection, so reflection phase method is more applicable. Moreover, we can call the overlap of these three as the bandwidth of the structure, to be sure that we have selected the right working frequency for the antenna.

5. Low Profile Dipole Antenna with EBG Ground Plane

In many communication devices, it is more desirable to have a low profile antenna. In these antennas the overall height is usually less than one tenth of the operating wavelength [1]. Besides, in many antennas a metal plane is used as a reflector or ground plane [16]. This ground plane redirects one-half of the radiation into the opposite direction, improving the antenna gain by 3dB, and shielding objects on the other side [6], but it causes a limitation for the antenna's height. The antenna can't be too close to the metal plane because of the coupling effect. So a fundamental challenge is the coupling effect of the ground plane.

If we place a vertical antenna over a PEC surface as the ground plane, the electric current will be vertical to the plane, so the image current will be in the same direction and will reinforce the radiation of the original current. Thus, this antenna has good radiation efficiency, but it suffers from high height of antenna, due to the vertical placement. To realize a low profile configuration, it is better to put the antenna horizontally over the ground plane, but in this case, the problem will be the poor radiation efficiency because of 180° reflection phase of PEC. As it is mentioned in previous sections, the EBG surface has a variable reflection phase, and is capable of providing a constructive image current within a certain frequency band. So it can result in good radiation efficiency.

As Figure 11 shows, we have placed a dipole antenna horizontally over an EBG ground plane with 7×7 array of cells. The radius of the dipole is 0.125mm and the height of the dipole is 0.5mm, so the overall height of antenna structure is 1.5mm. In order to obtain a resonant condition

for a half-wave dipole at 12GHz, the physical length must be somewhat shorter than the free space half-wavelength [28]. To find the optimum length of dipole, it has been changed and each time return loss of the antenna is obtained. Results show that the best return loss is achieved by a dipole with length of 12mm. Return loss of this dipole antenna over mushroom-like and slot loaded EBG ground planes is shown in Figure 12.

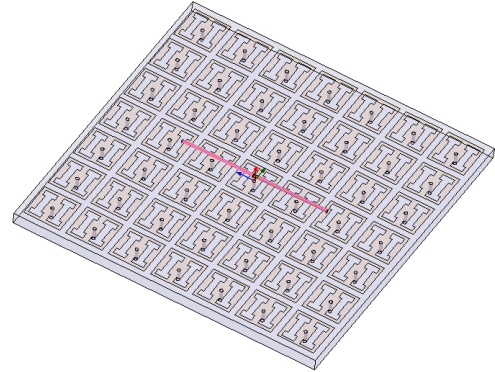


Fig. 11 Dipole antenna over EBG ground plane.

To study the effect of EBG structure first we place the dipole over a PEC ground plane of the same size as the EBG ones. The least return loss is -2.48dB at 11.58GHz, as it is shown in Figure 12. Then, we have used the mushroom-like EBG surface. In this case, the antenna has a return loss of -22.67dB at 12.64GHz. Finally, by replacing the mushroom-like EBG with the slot loaded structure, the antenna has showed the resonant frequency of 11.88GHz, and in this frequency return loss is -36.35dB.

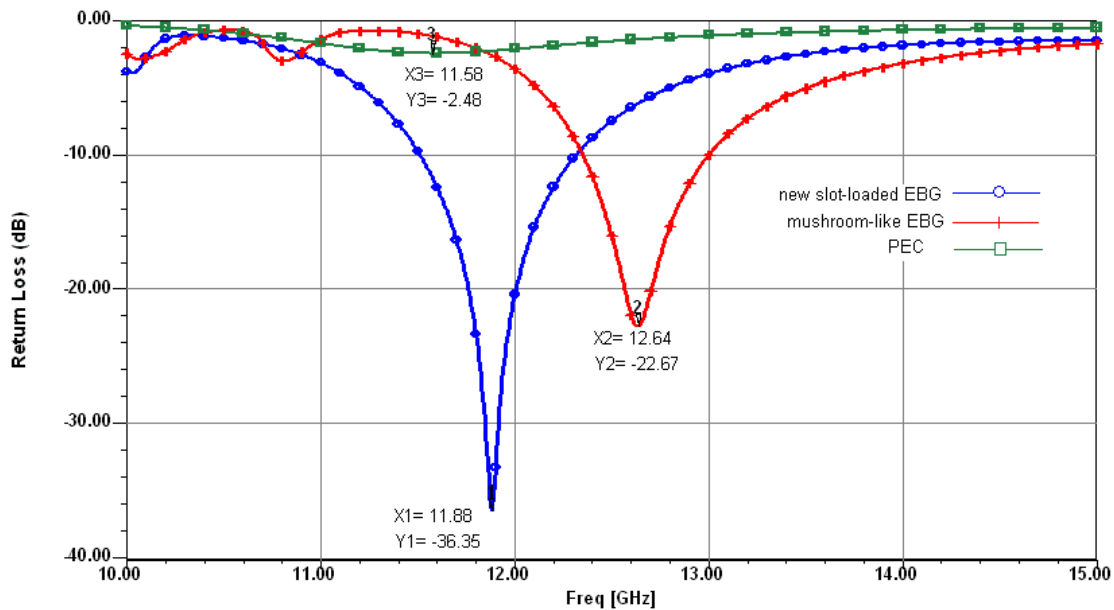


Fig. 12 Comparison of antenna return loss with mushroom-like EBG (P=w+g=3.5mm), slot-loaded EBG, and PEC ground planes.

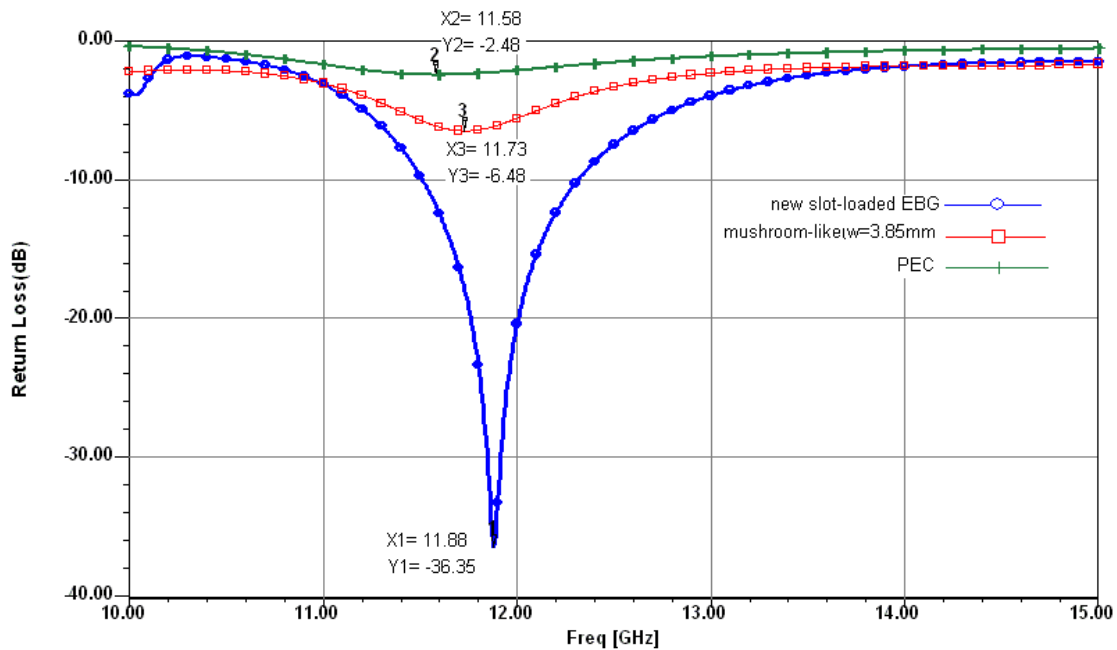


Fig. 13 Comparison of antenna return loss with mushroom-like EBG ($P=w+g=4.35\text{mm}$), slot-loaded EBG and PEC ground planes.

It is clear that using EBG ground planes have improved the return loss of antenna, and this improvement is more considerable for the slot loaded surface. By using the slot loaded EBG, we have 33.87dB improvement in antenna return loss in comparison to the PEC ground plane, and 13.68dB increase in comparison to the conventional mushroom-like structure.

The input-match frequency band of antenna is defined as the region where the antenna has a good return loss, usually less than -10dB. Regarding Figure 12, this bandwidth which can't be achieved by PEC ground plane, is 5.14% for the mushroom-like EBG and 6.82% for the slot loaded EBG.

As it is discussed in the previous sections, a mushroom-like EBG with the period of 4.35mm has the same frequency response as the novel slot loaded EBG structure. We have compared them as the ground plane of dipole antenna, too. Because of greater patch size of this mushroom-like cell, we used a 5×5 array to preserve the overall size of ground plane. The antenna return loss is depicted in Figure 13, and it is compared with the slot loaded and PEC ground planes. By this structure, the resonant frequency of antennas is almost the same, but the antenna has the minimum return loss of -6.48dB at 11.73GHz, and the input match frequency bandwidth is not accessible. Thus, it is not a good substitute for the novel slot loaded EBG structure, since the performance of the slot loaded surface is better. The results of return loss curves for different types of ground planes are summarized in Table 3.

Table 3: Comparison of performance of four different ground planes

Ground Plane Type	Resonant frequency (GHz)	Minimum return loss (dB)	Bandwidth
Novel slot loaded ($P=3.5\text{m}$)	11.88	-36.35	6.82%
Mushroom-like ($P=3.5\text{mm}$)	12.64	-22.67	5.14%
Mushroom-like ($P=4.35\text{mm}$)	11.73	-6.48	0%
PEC ($25 \times 25\text{mm}$)	11.58	-2.48	0%

Poor return loss of the PEC ground plane is due to 180° reflection phase and reverse image current, while using EBG ground plane, radiation of antenna has improved because of desirable reflection phase and surface wave frequency band gap. Figure 14 shows surface current density at resonant frequency. In EBG structure, surface current has been reduced because of its frequency band gap. Moreover, According to lower frequency band of the slot loaded EBG surface, it has a smaller cell size in comparison to mushroom-like EBG. The advantage of compactness makes this new EBG structure a promising candidate in practical applications.

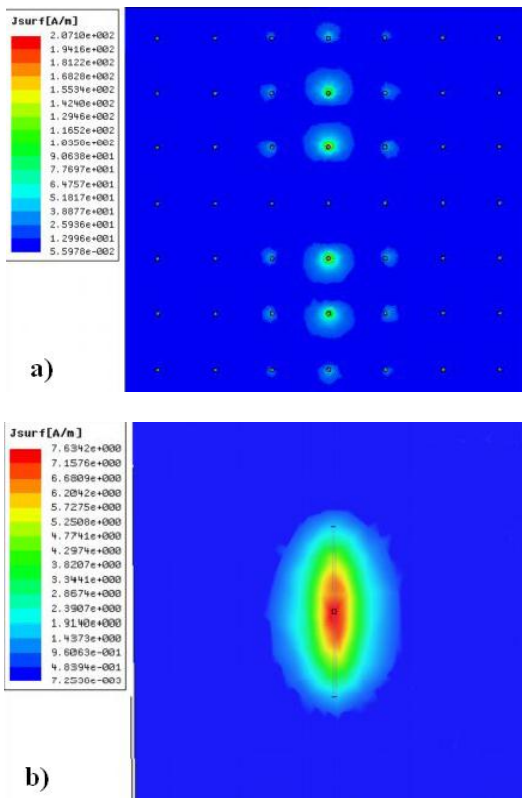


Fig. 14 Surface current density: a) EBG, and b) PEC ground planes.

6. Conclusions

In this paper, we have studied the properties of EBG structures, and have presented a novel slot loaded EBG. Its reflection phase and transmission characteristics are derived and compared with conventional mushroom-like EBG surface. Simulation results show that in-phase reflection frequency of this slot loaded EBG is 15.3% lower than mushroom-like EBG structure of the same size, and decreases from 17GHz to 14.4GHz. So the designed EBG is a compact structure and is a proper candidate in practical applications. Besides, we have used EBG structures to design a low profile antenna. These structures have been used as the ground plane to improve radiation of a low profile dipole antenna. Although both mushroom-like and slot loaded structures improve the return loss, the novel slot loaded EBG has better results. Using this slot loaded EBG surface, the antenna return loss decreases more than 13.68dB in comparison with conventional mushroom-like EBG of the same size, and 33.87dB in comparison with PEC ground plane. Moreover, the input-match frequency band of antenna is improved by 1.68% by replacing the mushroom-like EBG ground plane of the same size with the novel slot loaded EBG structure.

Acknowledgments

The authors would like to acknowledge the assistance and financial support provided by the Semnan University.

References

- [1] F. Yang, and Y. Rahmat-samii, *Electromagnetic band gap structures in antenna engineering*, Cambridge University Press, 2008.
- [2] D.Y. Shchegolkov, C.E. Heath, and E.I. Simakov, "Low loss metal diplexer and combiner based on a photonic band gap channel-drop filter at 109 GHz," *Progress In Electromagnetics Research*, PIER 111, 2011, pp. 197-212.
- [3] T.-N. Chang, and J.-H. Jiang, "Enhance gain and bandwidth of circularly polarized microstrip patch antenna using gap-coupled method," *Progress In Electromagnetics Research*, PIER 96, 2009, pp. 127-139.
- [4] F. Yang and Y. Rahmat-Samii, "Wire antenna on an EBG ground plane vs. patch antenna: A comparative study on low profile antennas," *URSI Electromagnetic Theory Symposium*, Ottawa, Canada, July 2007.
- [5] D. Zarifi, H. Oraizi, and M. Soleimani, "Improved Performance of Circularly Polarized Antenna Using Semi-Planar Chiral Metamaterial Covers," *Progress In Electromagnetics Research*, PIER 123, 2012, pp.337-354.
- [6] D. Sievenpiper, L. Zhang, R.F.J. Broas, N.G. Alexopolus, and E. Yablonovitch, "High-impedance electromagnetic surfaces with a forbidden frequency band," *IEEE Trans. Microwave Theory Tech.*, Vol. 47, 1999, pp. 2059-2074.
- [7] M. Rezaei Abkenar, P. Rezaei, and R. Narimani, "Design of a slot-loaded EBG surface for a low profile antenna," *IEEE AP-S Int. Symp. on Antennas and Propagation and USNC/URSI National Radio Science Meeting*, July 2010.
- [8] M. Rezaei Abkenar, and P. Rezaei, "Design of a compact slot-loaded EBG surface and its application in a low-profile antenna," *4th Int. Congress on Advanced Electromagnetic Materials in Microwaves and Optics*, 2010, pp. 800-802.
- [9] M. Rezaei Abkenar, and P. Rezaei, "Design of a novel EBG structure and its application for improving performance of a low profile antenna," *19th Iranian Conference on Electrical Engineering*, 2011, pp. 3020-3024.
- [10] M. Rezaei Abkenar, P. Rezaei, and R. Narimani, "Using mushroom-like EBG ground plane for improving radiation in low profile dipole antenna," *2010 URSI Int. Symp. on Electromagnetic Theory*, 2010, pp. 635-638.
- [11] "HFSS Release 11.0," Ansoft Corp., 2005.
- [12] "CST Reference Manual." Darmstadt, Germany, Computer Simulation Technology, 2008.
- [13] D.K. Cheng, *Field and wave electromagnetics*, 2nd Ed., Addison-Wesley, 1992.
- [14] R. Collin, *Field theory of guided waves*, 2nd Ed., IEEE Press, New York, 1991.
- [15] N. Ashcroft, and N. Mermin, *Solid state physics*, Saunders College Publishing, Orlando, 1976.
- [16] C.A. Balanis, *Antenna Theory: Analysis and Design*, 3rd Ed., John Wiley & Sons, New York, 2005.
- [17] S. Ramo, J.R. Whinnery, and T. Van Duzer, *Fields and waves in communication electronics*, 2nd Ed., John Wiley and Sons, New York, 1984.

- [18] D. Sievenpiper, "High-impedance electromagnetic surfaces," Ph.D. dissertation at University of California, Los Angeles, 1999.
- [19] F. Yang, and Y. Rahmat-Samii, "Polarization dependent electromagnetic band gap (PDEBG) structures: designs and applications," *Microwave Optical Tech. Lett.*, Vol. 41, No. 6, 2004, pp. 439-444.
- [20] S.M. Moghadasi, A.R. Attari, and M.M. Mirsalehi, "Compact and wideband 1-D mushroom-like EBG filters," *Progress In Electromagnetics Research, PIER* 83, 2008, pp. 323-333.
- [21] L. Yang, Z.H. Feng, F.L. Chen, and M.Y. Fan, "A novel compact electromagnetic band-gap (EBG) structure and its application in microstrip antenna arrays," *IEEE MTT-S Int. Microwave Symp. Dig.*, 2004, pp. 1635-1638.
- [22] F. Xu, Z. X. Wang, X. Chen, and X.-A. Wang, "Dual Band-Notched UWB Antenna Based on Spiral Electromagnetic-Bandgap Structure," *Progress In Electromagnetics Research B, PIER B* 39, 2012, pp. 393-409.
- [23] Y. Gou, Q. Wu and J. Hua, "Design of A Bandwidth Extended and Compact Microstrip Antenna Based on CRLH TL with Slot Loaded," *Microwave Conference Proceedings (APMC), 2011 Asia-Pacific*, 2011, pp. 1762-1765.
- [24] R. Remski, "Analysis of photonic band gap surfaces using Ansoft HFSS," *Microwave Journal*, Sept. 2000.
- [25] F. Yang, and Y. Rahmat-Samii, "Reflection phase characterizations of the EBG ground plane for low profile wire antenna applications," *IEEE Trans. Antennas Propagat.*, Vol. 51, No. 10, 2003, pp. 2691-2703.
- [26] R. Gonzalo, P. Maagt, and M. Sorolla, "Enhanced Patch-Antenna Performance by Suppressing Surface Waves Using Photonic-Bandgap Substrates," *IEEE Trans. Microwave Theory Tech.*, vol. 47, pp. 2131-8, 1999.
- [27] F. Yang, K. Ma, Y. Qian, and T. Itoh, "A novel TEM waveguide using uniplanar compact photonic-bandgap (UC-PBG) structure," *IEEE Trans. On Microwave Theory and Tech.*, Vol. 47, No. 11, 1999, pp. 2092-2098.
- [28] W.L. Stutzman, and G.A. Thiele, *Antenna theory and design*, 2nd Ed., John Wiley and Sons, New York, 1998.

Masoumeh Rezaei Abkenar was born in Tehran, Iran, in 1983. She received the B.S. degree in Electronic Engineering from Khaje Nasir Toosi University of Technology, Tehran, Iran, and the M.S. degree from Semnan University, Semnan, Iran, in 2006 and 2010, respectively. Her research interests include low-profile printed and patch antennas for wireless communication, miniaturized and multiband antennas, metamaterials and EBG structures interactions with antennas and RF passive components.

Pejman Rezaei was born in Tehran, Iran, in 1977. He received the B.S. degree in Electrical-Communication Engineering from Communication Faculty, Tehran, Iran, in 2000, and the M.S. and Ph.D. degrees from Tarbiat Modarres University, Tehran, Iran, in 2002 and 2007, respectively. Currently, he is assistant professor in the Semnan University, Semnan, Iran. His current research interests are Electromagnetics theory, metamaterial structure, theory and design of antenna, wave propagation, and satellite communication.

